



## Historical and future anthropogenic warming effects on the year 2015 droughts, fires and fire emissions of CO<sub>2</sub> and PM<sub>2.5</sub> in equatorial Asia

Hideo Shiogama<sup>1</sup>, Ryuichi Hirata<sup>1</sup>, Tomoko Hasegawa<sup>2</sup>, Shinichiro Fujimori<sup>3</sup>, Noriko Ishizaki<sup>1</sup>, Satoru Chatani<sup>1</sup>, Masahiro  
5 Watanabe<sup>4</sup>, Daniel Mitchell<sup>5</sup>, Y. T. Eunice Lo<sup>5</sup>

<sup>1</sup>National Institute for Environmental Studies, 16-2 Onogawa, Tsukuba, Ibaraki 305-8506, Japan

<sup>2</sup>College of Science and Engineering, Ritsumeikan University, 1-1-1 Noji-higashi, Kusatsu, Shiga 525-8577, Japan

<sup>3</sup>Department Environmental Engineering, Graduate School of Engineering, Kyoto University, Kyoto 615-8540 Japan  
10 <sup>4</sup>Atmosphere and Ocean Research Institute, University of Tokyo, 5-1-5 Kashiwanoha, Kashiwa, Chiba 277-8564, Japan

<sup>5</sup>School of Geographical Sciences, University of Bristol, University Road, Bristol BS8 1SS, United Kingdom

Correspondence to: Hideo Shiogama ([shiogama.hideo@nies.go.jp](mailto:shiogama.hideo@nies.go.jp))

**Abstract.** In 2015, El Niño caused severe droughts in equatorial Asia (EA). The severe droughts enhanced fire activities in  
15 the dry seasons, leading to massive fire emissions of CO<sub>2</sub> and aerosols. Using large event attribution ensembles of the MIROC5  
atmospheric global climate model, we suggest that historical anthropogenic warming increased the chances of meteorological  
droughts exceeding the 2015 observations in the EA area. Large probability increases in stronger droughts than the 2015 event  
are found in the ensemble simulations of 1.5°C and 2.0°C global warming according to the Paris Agreement goals. Further  
drying is projected in the 3.0°C ensemble.

20 We combine these experiments and empirical functions between precipitation, burned area, and fire emissions of CO<sub>2</sub> and  
PM<sub>2.5</sub>. Increases in the chances of the burned area and the emissions of CO<sub>2</sub> and PM<sub>2.5</sub> exceeding the 2015 observations due  
to anthropogenic climate change in the past are not significant. In contrast, there are significant increases in the burned area  
and CO<sub>2</sub> and PM<sub>2.5</sub> emissions even if the 1.5°C and 2.0°C goals are achieved. If global warming reaches 3.0°C, as is expected  
from the current mitigation policies of nations, the chances of the burned area, CO<sub>2</sub> and PM<sub>2.5</sub> emissions exceeding the 2015  
25 observed values become approximately 100%, at least in the single model ensembles.

We also compare changes in fire CO<sub>2</sub> emissions due to climate changes and the land-use CO<sub>2</sub> emission scenarios of five  
shared socio-economic pathways, where the climate change effects on fire are not considered. There are two main implications.  
First, in a national policy context, future EA climate policy will need to consider these climate change effects regarding both  
mitigation and adaptation aspects. Second, the consideration of fire increases would change global CO<sub>2</sub> emissions and the  
30 mitigation strategy, which suggests that future climate change mitigation studies should take these factors into account.

### 1 Introduction

In 2015/2016, a major El Niño event enhanced severe drought in equatorial Asia (EA, the area denoted by the black box in  
Figs. 1a-c) during the dry season. Tropical peatlands in EA contain tremendous soil organic carbon (Page et al., 2011) and  
huge biomass (Baccini et al., 2012, 2017; Saatchi et al., 2011). Coupled with anthropogenic land-use change (e.g., expansion  
35 of oil palm plantations on peatlands), the severe drought increased fire activities in forests and peatlands, leading to wide-  
ranging disasters on economy (at least 16.1 billion USD for Indonesia), ecology and human health (Taufik et al., 2017; World  
Bank 2016, Hartmann et al., 2018). The fires enhanced the emissions of CO<sub>2</sub> and aerosols (Yin et al., 2016; Field et al., 2016;  
Koplitz et al., 2016). The estimated 2015 CO<sub>2</sub>-equivalent biomass burning emissions for all Indonesia (1.5 billion metric tons  
CO<sub>2</sub>) were between the 2013 annual fossil fuel CO<sub>2</sub> emissions of Japan and India (Field et al., 2016). The massive emissions



40 of ozone precursors and aerosols including fine (<2.5 micrometre) particulate matter ( $PM_{2.5}$ ) caused severe haze across much of EA (Field et al., 2016), resulting in the excess deaths of approximately 100,300 people (Kopplitz et al., 2016).

In a previous study (Lestari et al., 2014), we suggested that recent fire events in Sumatra were exacerbated by human-induced drying trends by analysing two sets of historical simulations of the MIROC5 atmospheric global climate model (AGCM) (Watanabe et al., 2010) with and without anthropogenic warming. Lestari et al. (2014) and Yin et al. (2016) projected future  
45 increases in the frequencies of droughts and fires with analyses of the Coupled Model Intercomparison Project Phase 5 (CMIP5) model ensembles (Taylor et al., 2012).

This study has three aims. First, we examine whether historical climate changes increased the probabilities of drought, fire, fire emissions of  $CO_2$  and  $PM_{2.5}$  during the June–November dry season of 2015. We use a probabilistic event attribution approach based on ensembles of the MIROC5 AGCM with and without anthropogenic warming that are larger than Lestari et al. (2014): 100 and 10 members in this study and Lestari et al. (2014), respectively. These probabilistic event attribution  
50 experiments of MIROC5 have been used for many attribution studies of single extreme events, e.g., the 2010 drought in the southern Amazon region (Shiogama et al., 2013), the 2013 heat wave in the southwestern United States (Shiogama et al., 2013), the summer 2013 heat wave in Korea (Kim et al., 2018) and the unexpected disruption of the stratospheric quasi-biennial oscillation in February 2016 (Hirota et al., 2018).

55 Second, we examine how the probabilities of drought, fire and fire emissions of  $CO_2$  and  $PM_{2.5}$  would change when a major El Niño event similar to the one in 2015 occurs under at 1.5°C and 2.0°C warmed climate. We analyse a large (100-member) ensembles of the MIROC5 AGCM under the Half a degree Additional warming, Prognosis and Projected Impacts (HAPPI) project (Mitchell et al., 2016, 2017, 2018; Shiogama et al., 2019). The Paris Agreement sets the 2°C long-term climate stabilization goal and moreover states pursuing 1.5 °C for stabilization (United Nations Framework Convention on Climate  
60 Change 2015). To inform climate policies, it is worthwhile to quantify differences in extreme events and the associated impacts in cases between the 1.5°C and 2.0°C goals. These MIROC5 HAPPI ensembles have been used, for example, to study the changes in extreme hot days (Wehner et al., 2018), extreme heat-related mortality (Mitchell et al., 2018), tropical rainy season length (Saeed et al., 2018) and global drought (Liu et al., 2018) at 1.5°C and 2.0°C global warming.

Third, we perform and analyse a large ensemble of a 3.0°C warmed climate. There is a significant “emissions gap”, which  
65 is the gap between where we are likely to be and where we need to be (United Nations Environment Programme 2018). The current mitigation policies of nations would lead to global warming of approximately 3.2°C (with a range of 2.9–3.4°C) by 2100 (United Nations Environment Programme 2018). Therefore it is worthwhile to compare changes in extreme events and impacts in cases in which the 1.5°C and 2.0°C goals are achieved or not.

By using the above ensembles, we answer the following questions:

- 70 (a) Has historical climate change significantly affected the probabilities of drought, fire and fire emissions of  $CO_2$  and  $PM_{2.5}$ ?
- (b) How do the probabilities of drought, fire and fire emissions in the 2015-like major El Niño year change if we can limit global warming to 1.5°C and 2.0°C? Adaptation investments are necessary to reduce the associated impacts.
- 75 (c) If we overshoot the 1.5°C and 2.0°C goals to the current trajectory of 3.0°C, how will drought, fire and fire emissions be altered? Comparisons of the results of 3.0°C and 2.0°C/1.5°C indicate the potential benefits of mitigation efforts to achieve the goals of the Paris Agreement.

Although socio-economic factors (e.g., conversions of forest and peatlands to agriculture and plantations of oil palm) are also important for fire activities (Marlier et al., 2013, 2015; Kim et al., 2015), we only examine the effects of climate change in this study. In sections 2 and 3, we describe the empirical functions and model simulations used in this study, respectively. In  
80 section 4 we examine changes in precipitation, fire and fire emissions. Finally, section 5 contains the conclusions.



## 2 Empirical functions

Figures 1a-c indicate the observed June-November 2015 mean anomalies in surface air temperature ( $\Delta T$ ), vertical pressure velocity at the 500-hPa level ( $\Delta\omega_{500}$ ) and precipitation ( $\Delta P$ ) relative to the 1979-2016 averages. ERA Interim reanalysis (ERA-I) data (Dee et al., 2011) is used for  $\Delta T$  and  $\Delta\omega_{500}$ . Global Precipitation Climatology Project (GPCP) data (Adler et al., 2003) is analysed for  $\Delta P$ . The largely positive  $\Delta T$  over the eastern tropical Pacific Ocean (i.e., El Niño) is related to substantial downward motion anomalies and negative precipitation anomalies over the EA region (the area shown by black rectangles in Figs. 1a-c). In the EA region, the negative precipitation anomalies are associated with the enhanced fire fraction, fire CO<sub>2</sub> emissions and fire PM<sub>2.5</sub> emissions estimated from Global Fire Emissions Database (GFED4s) (van der Werf et al., 2017) (Figs. 1d-f).

Previous studies found that fire activities and related emissions have non-linear relationships with precipitation anomalies and accumulated water deficits (Lestari et al., 2014; Spessa, et al. 2015; Yin et al., 2016; Field et al., 2016). Figure 2 shows the empirical relationships between the EA averaged precipitation anomalies (GPCP, divided by the standard deviation) and the EA cumulative burned area and fire CO<sub>2</sub> and PM<sub>2.5</sub> emissions (GFED4s) during 1979-2016. As precipitation decreases, the burned area, fire CO<sub>2</sub> and PM<sub>2.5</sub> emissions increase exponentially. We estimate the fitting curves (solid curves in Fig. 2) by using the following equation,

$$\ln(y) = a + b\Delta P, \quad (\text{Eq.1})$$

where  $y$  is the burned area, CO<sub>2</sub> emissions or PM<sub>2.5</sub> emissions, and  $a$  and  $b$  are the intercept and regression coefficient, respectively. The coefficients of determination ( $R^2$ ) are higher than 0.7. We also estimate the 10%-90% confidence intervals of the fitting curves by applying a 1000-time random sampling of the observed data.

## 3 Model simulations

We perform 10-member long-term (1979-2016) historical simulations (Hist-long) of the MIROC5 AGCM (Watanabe et al. 2010) forced by the observed sea surface temperature (SST) and anthropogenic and natural external forcing factors (Shiogama et al., 2013; 2014). The MIROC5 model has good hindcast skill regarding interannual variability in the EA-averaged  $\Delta P$  and  $\Delta\omega_{500}$ : the correlations of the time series of  $\Delta P$  and  $\Delta\omega_{500}$  between the observations and the ensemble averages of the MIROC5 simulations are 0.90 and 0.87, respectively (Figs. 3a-b). Here, the  $\Delta P$  and  $\Delta\omega_{500}$  of each ensemble member are normalized by the corresponding standard deviation values, respectively. The precipitation and vertical motion anomalies are closely related to the Nino 3.4 SST (an index of El Niño Southern Oscillation) in the observations, and the MIROC5 model represents these relationships well (Figs. 3c-e).

To investigate whether historical anthropogenic climate change affected the precipitation anomalies during the 2015 El Niño event, we analyse the outputs of two large ensembles of factual historical-forcing (Hist) and counterfactual natural-forcing (Nat) of MIROC5 (100 members each) for June-November 2015 (Shiogama et al. 2013, 2014). These simulations are called “probabilistic event attribution” experiments, which contribute to “the International Climate and Ocean: Variability, Predictability and Change (CLIVAR) C20C+ Detection and Attribution Project (Stone et al. 2019)”. The Hist ensemble is forced by historical anthropogenic and natural external forcing factors plus observational data of SST and sea ice (HadISST, Rayner et al., 2003). The Nat ensemble is forced by historical natural forcing factors and hypothetical “natural” SST and sea ice patterns where long-term anthropogenic signals were removed. Please note that both the Hist and Nat ensembles have the same spatial SST patterns as the 2015 El Niño event, but the prescribed long-term warming anomalies in SST are different between each other. Please see Shiogama et al. (2013; 2014) and Stone et al. (2019) for details regarding the experimental design.



We also analyse the 100 member ensembles during 2006-2015 with 1.5°C and 2.0°C warming relative to preindustrial levels. We performed those experiments to contribute to the HAPPI project (Mitchell et al. 2016, 2017, 2018; Shiogama et al. 2019). These future simulations have the same SST patterns as the 2015 El Niño event but the prescribed long-term warming anomalies in SST are added (sea ice and the anthropogenic agents are also changed) (Figs. 4-5). Please see Mitchell et al. (2017) for details regarding the experimental design.

Furthermore, we run the 100-member 3.0°C ensemble as an extension to the HAPPI project. Following the original HAPPI methodology, we add SST and sea ice concentration anomalies that represent additional warming in a 3°C world as compared to preindustrial values. The SST anomalies (Fig. 4 bottom panel) are changes in the CMIP5 multi-model mean SST for each month, between the decadal average of 2006-2015 in representative concentration pathway 8.5 (RCP8.5) and the decadal average of 2091-2100 in a combined scenario of RCP4.5 and RCP8.5, i.e.,  $0.686 \times \text{RCP4.5} + 0.314 \times \text{RCP8.5}$  (Lo et al. 2019). The CMIP5 multi-model mean global mean temperature in 2091-2100 is approximately 3°C warmer than the 1861-1880 mean in this combined scenario; hence, this scenario describes 3°C global warming above preindustrial levels. For the sea ice concentration anomalies, the HAPPI approach is to apply a linear sea ice-SST relationship estimated from observations to HAPPI SST anomalies (Mitchell et al., 2017). Here, we find the coefficients of this linear relationship from pre-existing 1.5°C and 2°C SST and sea ice anomalies. We apply this relationship to the 3°C SST anomalies to estimate the sea ice concentration anomalies, which are then added to the observed 2006-2015 data (see Mitchell et al., 2017). Figure 5 shows the sea ice concentrations in both hemispheres in the 1.5°C, 2°C and 3°C experiments. The same weightings for RCP4.5 and RCP8.5 in the combined scenario equivalent to 3°C warming are also applied to anthropogenic radiative forcing. This study is the first to report results from the HAPPI extension using MIROC5.

To compute the normalized values of EA-averaged  $\Delta P$  and  $\Delta\omega_{500}$  of the Hist, Nat, 1.5°C, 2.0°C and 3.0°C runs, we subtract a long-term mean value of a given single member of Hist-long, and divide anomalies by the standard deviation value of that Hist-long member. This normalization process enables us to produce  $100 \times 10 = 1000$  samples of normalized  $\Delta P$  and  $\Delta\omega_{500}$  data for each of the Hist, Nat, 1.5°C, 2.0°C and 3.0°C ensembles.

145

#### 4 Changes in precipitation, fire and fire emissions

The difference patterns of surface air temperature ( $\approx$  prescribed SST difference patterns over the ocean) in Hist-Nat, 1.5°C-Nat, 2.0°C-Nat and 3.0°C-Nat have greater warming in the Nino 3.4 region than the tropical (30°S-30°N) ocean averaged values (Fig. 6). The relatively high warming in the Nino 3.4 region accompanies downward motion anomalies in the EA region (Fig. 7a), enhancing negative precipitation anomalies when El Niño occurs (Figs. 7b). It should be noted that the prescribed SST difference between the Nino 3.4 region and the tropical ocean mean is larger in the 1.5°C runs than in the 2.0°C runs. As a result, the amplitude of negative precipitation in the 1.5°C runs is slightly greater than that in the 2.0°C runs, at least in these ensembles.

Historical anthropogenic climate change has significantly increased the chance of  $\Delta P$  being more negative than the observed value from 2% (1-4%) to 9% (6-14%) (Fig. 8a). The values in parentheses indicate the 10-90% confidence interval estimated by applying the 1000-time resampling. Even if the 1.5°C and 2.0°C goals of the Paris Agreement are achieved, the chance of exceeding the observed value significantly increases from 9% (6-14%) in Hist to 82% (76-87%) and 67% (60-74%), respectively. In the current trajectory of 3.0°C warming, the chance of exceeding the observed value becomes 93% (89-96%).

By combining the  $\Delta P$  of MIROC5 (Fig. 8a) and the empirical relationships of Fig.2, we assess historical and future changes in burned area, and fire emissions of CO<sub>2</sub> and PM<sub>2.5</sub> (Figs. 8b-d). We consider uncertainties by combining the 1000 resampled  $\Delta P$  values and 1000 random samples of the regression factors in Eq. 1. Historical anthropogenic drying has increased the probability of exceeding the observed values of the burned area (from 5% (0-18%) to 23% (3-52%)), CO<sub>2</sub> emissions (from 5%

160



(0-15%) to 23% (3-47%)), and  $PM_{2.5}$  emissions (from 2% (0-5%) to 24% (3-49%)), but these changes are not statistically significant due to the large uncertainties. In the 1.5°C, 2.0°C and 3.0°C runs, the chances of exceeding the observed values significantly increase for the burned area (93% (66-99%), 81% (50-95%) and 98% (84-100%), respectively),  $CO_2$  emissions (92% (72-98%), 81% (55-93%) and 98% (86-100%)), and  $PM_{2.5}$  emissions (93% (70-98%), 81% (54-94%) and 98% (85-100%)).

In the ensembles of Nat, Hist, 1.5°C, 2.0°C and 3.0°C, the probabilities of fire  $CO_2$  emissions exceeding the 2015  $CO_2$  emission of Japan due to fossil fuel consumptions (5<sup>th</sup> largest in the world) are 9% (1-20%), 34% (8-57%), 96% (81-99%), 87% (65-96%) and 100% (92-100%, indicating that more than half of the samples are 100%), respectively. While the historical change is not statistically significant, future increases are significant.

The above analyses focus on the year when the major El Niño event occurred. The cumulative probability function in Fig.9 indicates the 11-year (June-November 2006-2016) averaged fire  $CO_2$  emission in the 2.0°C runs, which include non-El Niño years. Although the 11-year averaged fire  $CO_2$  emissions (Fig. 9) is much less than those in the major El Niño year (Fig. 8c), the 11-year averaged emissions can have substantial implications for mitigation policies. We contextualize the estimated fire  $CO_2$  emission within the future emissions scenarios. The vertical lines in Fig. 9 are the year 2100 land-use  $CO_2$  emission scenarios (including fire emissions) for the East and South East Asia regions, except China and Japan in the five shared socio-economic pathway (SSP) scenarios that contribute to 6<sup>th</sup> assessment report of Intergovernmental Panel on Climate Change (Riahi et al. 2017, Fujimori et al. 2017). Here, as an example, we take an implementation of integrated assessment model, Asia-Pacific Integrated Model/Computable General Equilibrium (AIM/CGE) (Fujimori et al., 2012). The chances of exceeding the emissions of SSP1, 2, 3, 4 and 5 are 77% (70-84%), 34% (28-39%), 13% (10-18%), 37% (31-41%) and 77% (70-84%), respectively. Although these probability values highly depend on the SSP scenarios, the results are substantial in all the SSP scenarios. Because the  $CO_2$  emissions in the AIM/CGE model include a wider area and other emission sources than the EA fire emissions, this comparison is conservative. In the SSP simulations of AIM/CGE, fire  $CO_2$  emissions are computed by using functions of land-cover changes, and climate change effects on fires are not considered. It is suggested that implementing climate change effects on fire  $CO_2$  emissions in integrated assessment models can significantly affect the SSP emission pathways and studies of mitigation pathways, which in turn would be highly relevant to national and global climate policies.

190

## 5 Conclusions

By applying the probabilistic event attribution approach based on the MIROC5 AGCM ensembles, we suggested that historical anthropogenic warming had significantly increased the chance of severe meteorological drought exceeding the 2015 observations in the EA area during the 2015 major El Niño year (from 2% in Nat to 9% in Hist). By performing and analysing the HAPPI (1.5°C and 2.0°C warming) and HAPPI extension (3.0°C warming) runs, we showed that the probabilities of drought exceeding the 2015 observations will largely increase (82%, 67% and 93%, respectively).

Drying trends tend to exacerbate fire activities. By combining these experiments and the empirical functions, we also implied that historical anthropogenic drying had somewhat increased the chances of the burned area,  $CO_2$  emissions and  $PM_{2.5}$  emissions exceeding the 2015 observations, but those changes were not statistically significant. In contrast, if the 2.0°C goal is achieved, the chances of exceeding the observed values will substantially increase for the burned area (from 23% in Hist to 81% for 2.0°C),  $CO_2$  emissions (from 23% to 81%) and  $PM_{2.5}$  emissions (from 24% to 81%). The impacts of these changes on droughts, fire and fire emissions should be reduced by adaptation investments.

200



If we cannot limit global warming to 2.0°C and it reaches 3.0°C as expected from the current “emissions gap” (United Nations Environment Programme 2018), the chances of exceeding the observed values become 98% from 81% for 2°C for the  
205 burned area, CO<sub>2</sub> emissions and PM<sub>2.5</sub> emissions. These additional changes relative to 2.0°C indicate the effects of failure of mitigation policies. Conversely, these changes indicate the potential benefits of limiting the current trajectory of 3°C global warming to the Paris Agreement goals.

Forest-based climate mitigation has a key role in meeting the goals of the Paris Agreement (Grassi et al., 2017). We also suggested that changes in fire CO<sub>2</sub> emissions due to future warming can increase the need for modifying fire CO<sub>2</sub> emission  
210 scenarios for future climate projections. Although we focused on the influences of climate change on fires, land use and land cover changes are important factors. To avoid fire intensification due to drying climates, effective land management policies of protecting forests and peatlands are necessary (Marlier et al., 2015; Kim et al., 2015; Koplitz et al., 2016; World Bank 2016).

215

#### Acknowledgments

This study was supported by ERTDF 2-1702 (Environmental Restoration and Conservation Agency, Japan) and TOUGOU (MEXT, Japan). This research used the science gateway resources of the National Energy Research Scientific Computing Center, a DOE Office of Science User Facility supported by the Office of Science of the U.S. Department of Energy under  
220 contract no. DE-AC02-05CH11231. The MIROC5 simulations were performed using the Earth Simulator at JAMSTEC and the NEC SX at NIES.



## References

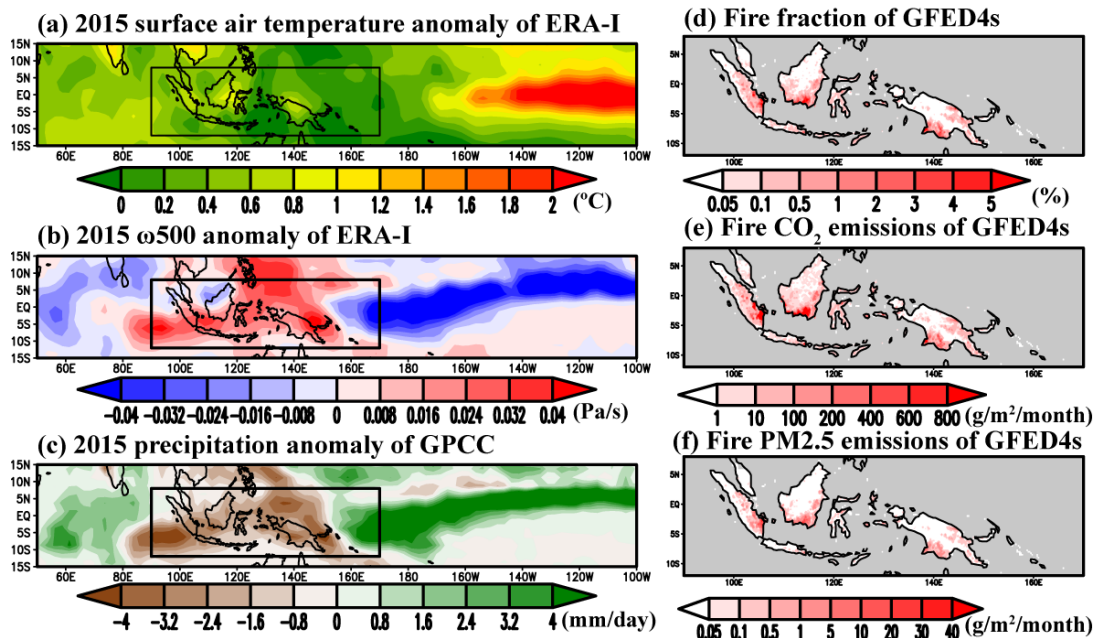
- 225 Adler, R. F., Huffman, G. J., Chang, A., Ferraro, R., Xie, P.-P., Janowiak, J., Rudolf, B., Schneider, U., Curtis, S., Bolvin, D., Gruber, A., Susskind, J., Arkin, P. and Nelkin, E.: The Version-2 Global Precipitation Climatology Project (GPCP) Monthly Precipitation Analysis (1979–Present), *J. Hydrometeorol.*, 4(6), 1147–1167, doi:10.1175/1525-7541, 2003.
- Baccini, A., Goetz, S.J., Walker, W.S., Laporte, N.T., Sun, M., Sulla-Menashe, D., Hackler, J., Beck, P. S. A., Dubayah, R., Friedl, M. A., Samanta, S., Houghton, R. A.: Estimated carbon dioxide emissions from tropical deforestation improved by carbon-density maps. *Nature Climate Change*, 2, 182-185, 2012.
- 230 Baccini, A., Walker, W., Carvalho, L., Farina, M., Sulla-Menashe, D., Houghton, R.A.: Tropical forests are a net carbon source based on aboveground measurements of gain and loss. *Science*, 358, 230-233, 2017.
- Dee, D. P., Uppala, S. M., Simmons, A. J., Berrisford, P., Poli, P., Kobayashi, S., Andrae, U., Balmaseda, M. A., Balsamo, G., Bauer, P., Bechtold, P., Beljaars, A. C. M., van de Berg, L., Bidlot, J., Bormann, N., Delsol, C., Dragani, R., Fuentes, M., Geer, A. J., Haimberger, L., Healy, S. B., Hersbach, H., Hólm, E. V., Isaksen, I., Kållberg, P., Köhler, M., Matricardi, M., McNally, A. P., Monge-Sanz, B. M., Morcrette, J. J., Park, B. K., Peubey, C., de Rosnay, P., Tavolato, C., Thépaut, J. N. and Vitart, F.: The ERA-Interim reanalysis: Configuration and performance of the data assimilation system, *Q. J. R. Meteorol. Soc.*, doi:10.1002/qj.828, 2011.
- 235 Field, R. D., van der Werf, G. R., Fanin, T., Fetzer, E. J., Fuller, R., Jethva, H., Levy, R., Livesey, N. J., Luo, M., Torres, O. and Worden, H. M.: Indonesian fire activity and smoke pollution in 2015 show persistent nonlinear sensitivity to El Niño-induced drought, *Proc. Natl. Acad. Sci.*, doi:10.1073/pnas.1524888113, 2016.
- Fujimori, S., Hasegawa, T., Masui, T., Takahashi, K., Herran, D. S., Dai, H., Hijioka, Y. and Kainuma, M.: SSP3: AIM implementation of Shared Socioeconomic Pathways, *Glob. Environ. Chang.*, doi:10.1016/j.gloenvcha.2016.06.009, 2017.
- Fujimori, S., Masui, T. and Matsuoka, Y.: AIM/CGE [basic] manual. Center for Social and Environmental Systems Research, NIES, Tsukuba, Japan, 2012.
- 245 Grassi, G., House, J., Dentener, F., Federici, S., Den Elzen, M. and Penman, J.: The key role of forests in meeting climate targets requires science for credible mitigation, *Nat. Clim. Chang.*, doi:10.1038/nclimate3227, 2017.
- Hartmann, F., Merten, J., Fink, M., Faust, H.: Indonesia's Fire Crisis 2015: A Twofold Perturbation on the Ground, *Pacific Geographies* #49, 4-11, doi:10.23791/490411, 2018
- 250 Hirota, N., Ogura, T., Tatebe, H., Shiogama, H., Kimoto, M. and Watanabe, M.: Roles of shallow convective moistening in the eastward propagation of the MJO in MIROC6, *J. Clim.*, doi:10.1175/JCLI-D-17-0246.1, 2018.
- Kim, P. S., Jacob, D. J., Mickley, L. J., Koplitz, S. N., Marlier, M. E., DeFries, R. S., Myers, S. S., Chew, B. N. and Mao, Y. H.: Sensitivity of population smoke exposure to fire locations in Equatorial Asia, *Atmos. Environ.*, 102, 11-17, doi:10.1016/j.atmosenv.2014.09.045, 2015.
- 255 Kim, Y. H., Min, S. K., Stone, D. A., Shiogama, H. and Wolski, P.: Multi-model event attribution of the summer 2013 heat wave in Korea, *Weather Clim. Extrem.*, doi:10.1016/j.wace.2018.03.004, 2018.
- Koplitz, S. N., Mickley, L. J., Marlier, M. E., Buonocore, J. J., Kim, P. S., Liu, T., Sulprizio, M. P., DeFries, R. S., Jacob, D. J., Schwartz, J., Pongsiri, M. and Myers, S. S.: Public health impacts of the severe haze in Equatorial Asia in September-October 2015: Demonstration of a new framework for informing fire management strategies to reduce downwind smoke exposure, *Environ. Res. Lett.*, doi:10.1088/1748-9326/11/9/094023, 2016.
- 260 Lestari, R. K., Watanabe, M., Imada, Y., Shiogama, H., Field, R. D., Takemura, T. and Kimoto, M.: Increasing potential of biomass burning over Sumatra, Indonesia induced by anthropogenic tropical warming, *Environ. Res. Lett.*, doi:10.1088/1748-9326/9/10/104010, 2014.



- Liu, W., Sun, F., Ho Lim, W., Zhang, J., Wang, H., Shiogama, H. and Zhang, Y.: Global drought and severe drought-Affected  
265 populations in 1.5 and 2°C warmer worlds, *Earth Syst. Dyn.*, doi:10.5194/esd-9-267-2018, 2018.
- Lo, Y.T.E, Mitchell, D.M., Gasparrini, A., Vicedo-Cabrera, A.M., Ebi, K.L., Frumhoff, P. C., Millar, R.J., Roberts, W., Sera,  
F., Sparrow, S., Uhe, P., Williams, G: Increasing mitigation ambition to meet the Paris Agreement’s temperature goal avoids  
substantial heat-related mortality in U.S. cities. *Science Advances*, 5(6), eaau4373, DOI: 10.1126/sciadv.aau4373, 2019
- Marlier, M. E., Defries, R. S., Kim, P. S., Gaveau, D. L. A., Koplitz, S. N., Jacob, D. J., Mickley, L. J., Margono, B. A. and  
270 Myers, S. S.: Regional air quality impacts of future fire emissions in Sumatra and Kalimantan, *Environ. Res. Lett.*,  
doi:10.1088/1748-9326/10/5/054010, 2015.
- Marlier, M. E., Defries, R. S., Voulgarakis, A., Kinney, P. L., Randerson, J. T., Shindell, D. T., Chen, Y. and Faluvegi, G.:  
El Niño and health risks from landscape fire emissions in southeast Asia, *Nat. Clim. Chang.*, doi:10.1038/nclimate1658,  
2013.
- 275 Mitchell, D., James, R., Forster, P. M., Betts, R. A., Shiogama, H. and Allen, M.: Realizing the impacts of a 1.5 °C warmer  
world, *Nat. Clim. Chang.*, doi:10.1038/nclimate3055, 2016.
- Mitchell, D., AchutaRao, K., Allen, M., Bethke, I., Beyerle, U., Ciavarella, A., Forster, P. M., Fuglestvedt, J., Gillett, N.,  
Haustein, K., Ingram, W., Iversen, T., Kharin, V., Klingaman, N., Massey, N., Fischer, E., Schleussner, C. F., Scinocca, J.,  
Seland, Ø., Shiogama, H., Shuckburgh, E., Sparrow, S., Stone, D., Uhe, P., Wallom, D., Wehner, M. and Zaaboul, R.:  
280 Half a degree additional warming, prognosis and projected impacts (HAPPI): Background and experimental design,  
*Geosci. Model Dev.*, doi:10.5194/gmd-10-571-2017, 2017.
- Mitchell, D., Heavyside, C., Schaller, N., Allen, M., Ebi, K. L., Fischer, E. M., Gasparrini, A., Harrington, L., Kharin, V.,  
Shiogama, H., Sillmann, J., Sippel, S. and Vardoulakis, S.: Extreme heat-related mortality avoided under Paris Agreement  
goals, *Nat. Clim. Chang.*, doi:10.1038/s41558-018-0210-1, 2018.
- 285 Page, S.E., Rieley, J.O., Banks C.J.: Global and regional importance of the tropical peatland carbon pool. *Global Change  
Biology*, 17, 798-818, 2011.
- Riahi, K., van Vuuren, D. P., Kriegler, E., Edmonds, J., O’Neill, B. C., Fujimori, S., Bauer, N., Calvin, K., Dellink, R., Fricko,  
O., Lutz, W., Popp, A., Cuaresma, J. C., KC, S., Leimbach, M., Jiang, L., Kram, T., Rao, S., Emmerling, J., Ebi, K.,  
Hasegawa, T., Havlik, P., Humpenöder, F., Da Silva, L. A., Smith, S., Stehfest, E., Bosetti, V., Eom, J., Gernaat, D., Masui,  
290 T., Rogelj, J., Strefler, J., Drouet, L., Krey, V., Luderer, G., Harmsen, M., Takahashi, K., Baumstark, L., Doelman, J. C.,  
Kainuma, M., Klimont, Z., Marangoni, G., Lotze-Campen, H., Obersteiner, M., Tabeau, A. and Tavoni, M.: The Shared  
Socioeconomic Pathways and their energy, land use, and greenhouse gas emissions implications: An overview, *Glob.  
Environ. Chang.*, doi:10.1016/j.gloenvcha.2016.05.009, 2017.
- Saatchi, S.S., Harris, N.L., Brown, S., Lefsky, M., Mitchard, E.T., Salas, W., Zutta, B.R., Buermann, W., Lewis, S. L., Hagen,  
295 S., Petrova, S., White, L., Silman, M., Morel, A.: Benchmark map of forest carbon stocks in tropical regions across three  
continents. *Proc Natl Acad Sci U S A*, 108: 9899-904, 2011.
- Saeed, F., Bethke, I., Fischer, E., Legutke, S., Shiogama, H., Stone, D. A. and Schleussner, C. F.: Robust changes in tropical  
rainy season length at 1.5 °C and 2 °C, *Environ. Res. Lett.*, doi:10.1088/1748-9326/aab797, 2018.
- Shiogama, H, T Hasegawa, S Fujimori, D Murakami, K Takahashi, K Tanaka, S Emori, I Kubota, M Abe, Y Imada, M  
300 Watanabe, D Mitchell, N Schaller, J Sillmann, E Fischer, J. F. Scinocca, I. Bethke, L Lierhammer J. Takakura, T. Trautmann,  
P. Döll, S. Ostberg, H. M. Schmied, F. Saeed, C.-F. Schleussner: Limiting global warming to 1.5°C will lower increases in  
inequalities of four hazard indicators of climate change. *Environ. Res. Lett.*, submitted, 2019
- Shiogama, H., Watanabe, M., Imada, Y., Mori, M., Ishii, M. and Kimoto, M.: An event attribution of the 2010 drought in the  
South Amazon region using the MIROC5 model, *Atmos. Sci. Lett.*, doi:10.1002/asl2.435, 2013.
- 305 Shiogama, H., Watanabe, M., Imada, Y., Mori, M., Kamae, Y., Ishii, M., Kimoto, M.: Attribution of the June–July 2013 heat  
wave in the southwestern United States. *SOLA*, 10, 122–126, doi:10.2151/sola.2014-025, 2014

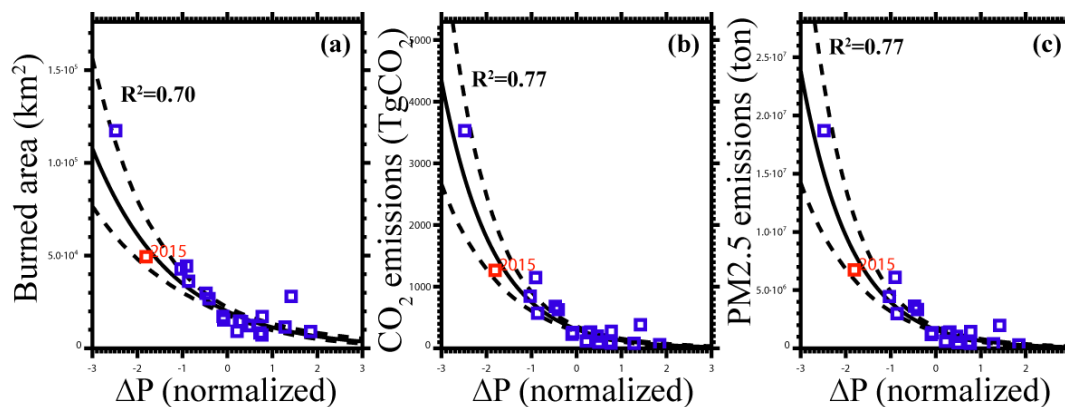


- Spessa, A. C., Field, R. D., Pappenberger, F., Langner, A., Englhart, S., Weber, U., Stockdale, T., Siegert, F., Kaiser, J. W. and Moore, J.: Seasonal forecasting of fire over Kalimantan, Indonesia, *Nat. Hazards Earth Syst. Sci.*, doi:10.5194/nhess-15-429-2015, 2015.
- 310 Stone, D. A., Christidis, N., Folland, C., Perkins-Kirkpatrick, S., Perlwitz, J., Shiogama, H., Wehner, M. F., Wolski, P., Cholia, S., Krishnan, H., Murray, D., Angéil, O., Beyerle, U., Ciavarella, A., Dittus, A., Quan, X. W. and Tadross, M.: Experiment design of the International CLIVAR C20C+ Detection and Attribution project, *Weather Clim. Extrem.*, doi:10.1016/j.wace.2019.100206, 2019.
- Taufik, M., Torfs, P. J. J. F., Uijlenhoet, R., Jones, P. D., Murdiyarto, D. and Van Lanen, H. A. J.: Amplification of wildfire area burnt by hydrological drought in the humid tropics, *Nat. Clim. Chang.*, doi:10.1038/nclimate3280, 2017.
- 315 Taylor, K. E., Stouffer, R. J. and Meehl, G. A.: An Overview of CMIP5 and Experimental Design, *Bull. Am. Meteorol. Soc.*, doi:10.1175/BAMS-D-11-00094, 2012.
- United Nations Environment Programme: Emissions Gap Report 2018, 2018
- United Nations Framework Convention on Climate Change: Adoption of the Paris Agreement FCCC/CP/2015/L.9/Rev.1,
- 320 2015
- Watanabe, M., Suzuki, T., O’Ishi, R., Komuro, Y., Watanabe, S., Emori, S., Takemura, T., Chikira, M., Ogura, T., Sekiguchi, M., Takata, K., Yamazaki, D., Yokohata, T., Nozawa, T., Hasumi, H., Tatebe, H. and Kimoto, M.: Improved climate simulation by MIROC5: Mean states, variability, and climate sensitivity, *J. Clim.*, doi:10.1175/2010JCLI3679.1, 2010.
- 325 Van Der Werf, G. R., Randerson, J. T., Giglio, L., Van Leeuwen, T. T., Chen, Y., Rogers, B. M., Mu, M., Van Marle, M. J. E., Morton, D. C., Collatz, G. J., Yokelson, R. J. and Kasibhatla, P. S.: Global fire emissions estimates during 1997-2016, *Earth Syst. Sci. Data*, 9(2), 697–720, doi:10.5194/essd-9-697-2017, 2017.
- Wehner, M., Stone, D., Mitchell, D., Shiogama, H., Fischer, E., Graff, L. S., Kharin, V. V., Lierhammer, L., Sanderson, B. and Krishnan, H.: Changes in extremely hot days under stabilized 1.5 and 2.0 °C global warming scenarios as simulated by
- 330 the HAPPI multi-model ensemble, *Earth Syst. Dyn.*, doi:10.5194/esd-9-299-2018, 2018.
- World Bank: The cost of fire: an economic analysis of Indonesia’s 2015 fire crisis (English). Indonesia sustainable landscapes knowledge; note no. 1. Washington, D.C. : World Bank Group, 2016
- Yin, Y., Ciais, P., Chevallier, F., van der Werf, G. R., Fanin, T., Broquet, G., Boesch, H., Cozic, A., Hauglustaine, D., Szopa, S. and Wang, Y.: Variability of fire carbon emissions in equatorial Asia and its nonlinear sensitivity to El Niño, *Geophys. Res. Lett.*, doi:10.1002/2016GL070971, 2016.
- 335

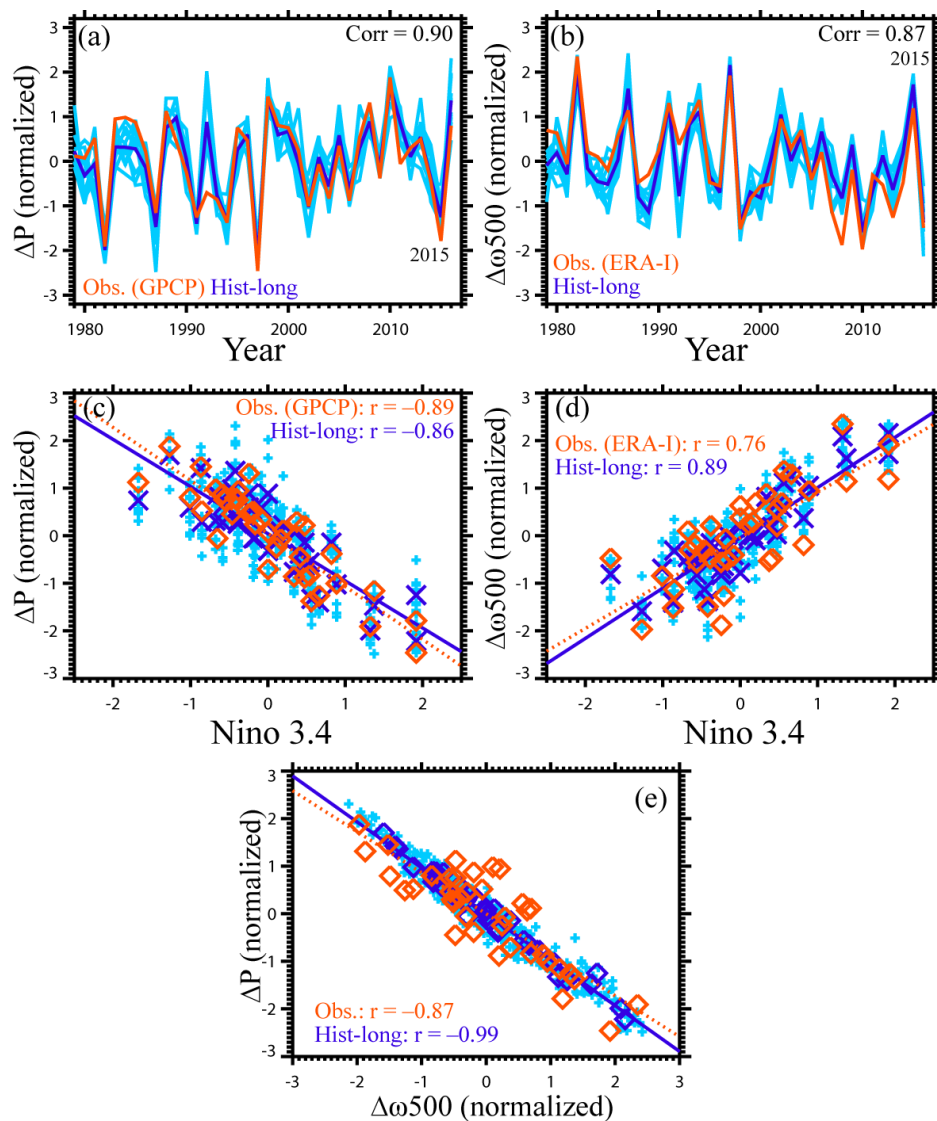


340 **Figure 1:** The observed climate conditions and fires. The June–November 2015 averaged anomalies of (a) surface air temperature (°C) and (b) vertical pressure velocity at the 500-hPa level (Pa<sup>-1</sup>, downward motions are positive) from ERA Interim reanalysis data (Dee et al. 2011) relative to the 1979–2016 mean. (c) The June–November 2015 averaged anomalies of precipitation from GPCP (Adler et al. 2003) (mm/day). The left panels indicate (d) fire fraction (%), (e) fire CO<sub>2</sub> emissions (gm<sup>-2</sup>month<sup>-1</sup>) and (f) fire PM<sub>2.5</sub> emissions from GFED4s (van der Werf et al. 2017) during June–November 2015.

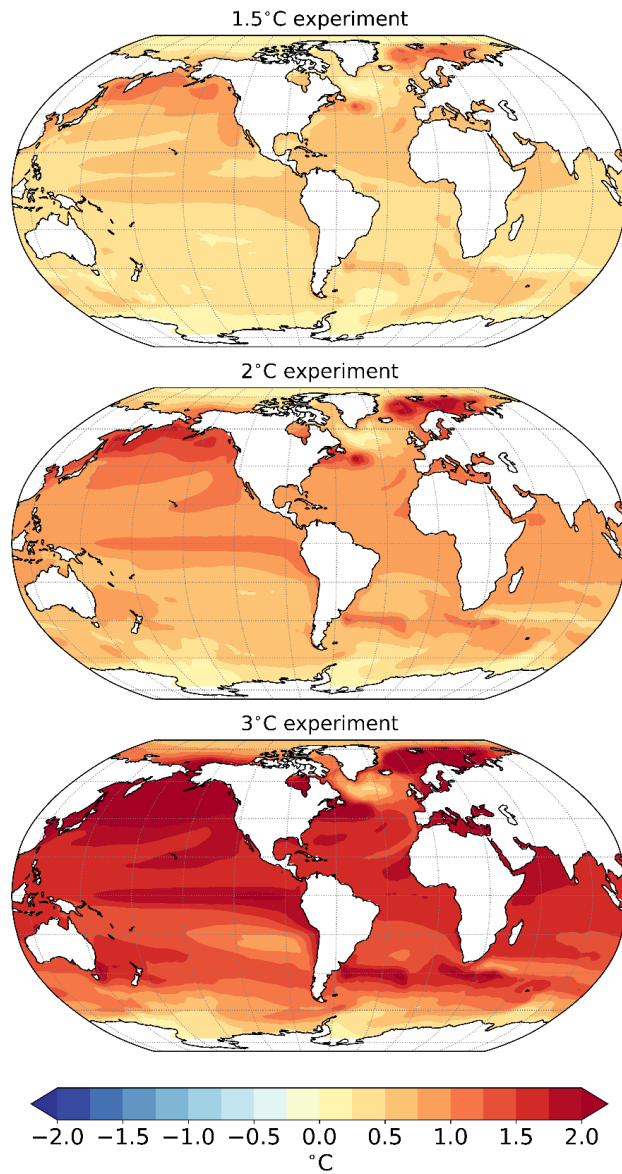
345



350 Figure 2: Empirical relationships between observed precipitation anomalies and fires, and fire emissions in the EA area. The horizontal axes are the normalized June-November mean precipitation anomalies (no unit) of GPCP during 1979-2016. The vertical axes denote (a) burned area ( $\text{km}^2$ ), (b)  $\text{CO}_2$  emissions ( $\text{TgCO}_2$ ) and (c)  $\text{PM}_{2.5}$  emissions (ton) of GFED4s, respectively. The year 2015 values are indicated by red squares. Solid and dashed lines indicate the best estimates and 10-90% confidence intervals of the fitting curves, Eq .1, respectively.



355 **Figure 3:** Evaluations of the MIROC5 simulations of the EA averaged precipitation and vertical air motions. Top panels show the  
 normalized June–November mean time series of (a)  $\Delta P$  (no unit) and (b)  $\Delta\omega_{500}$  (no unit), respectively. Red lines are the  
 observations. Light blue lines are the 10 ensemble members of Hist-long, and blue lines are the ensemble mean. The other panels  
 are scatter plots of (c)  $\Delta P$  and the Nino 3.4 index ( $^{\circ}C$ ), (d)  $\Delta\omega_{500}$  and the Nino 3.4 index and (e)  $\Delta P$  and  $\Delta\omega_{500}$ . Red diamonds are  
 the observed values. Small light blue crosses are the 10 ensemble members of Hist-long, and large blue crosses indicate the  
 ensemble mean values. The red and blue lines indicate the regression lines of the observations and the ensemble averages of Hist-  
 360 long, respectively.



365 **Figure 4: The 2006-2015 mean SST differences (°C) between (top) 1.5 °C and Hist, (middle) 2.0 °C and Hist and (bottom) 3.0 °C and Hist.**

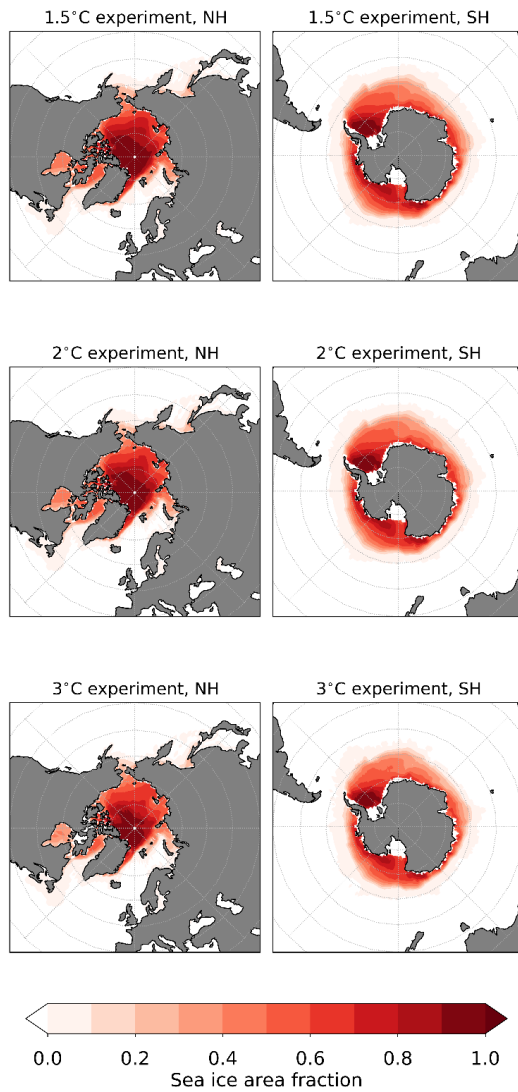


**Figure 5:** The 2006-2015 mean sea ice area fraction of (top) 1.5 °C, (middle) 2.0 °C and (bottom) 3.0 °C for (left and right) the Northern and Southern Hemispheres, respectively.

370

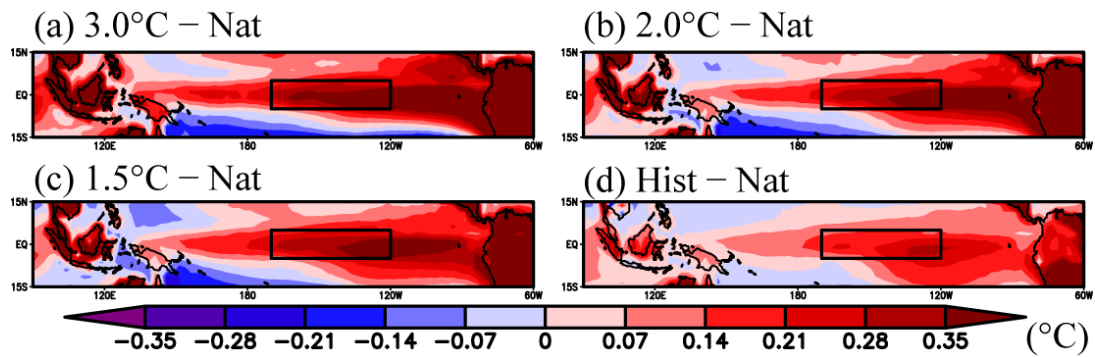
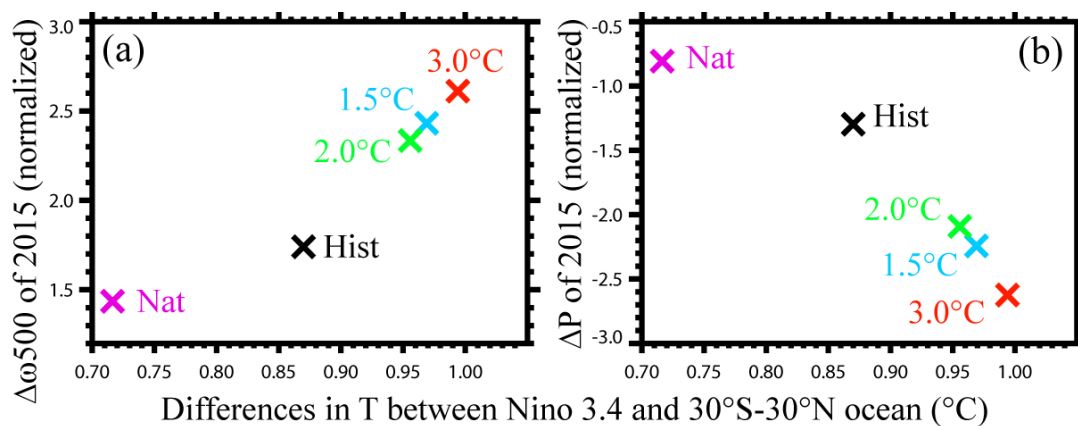
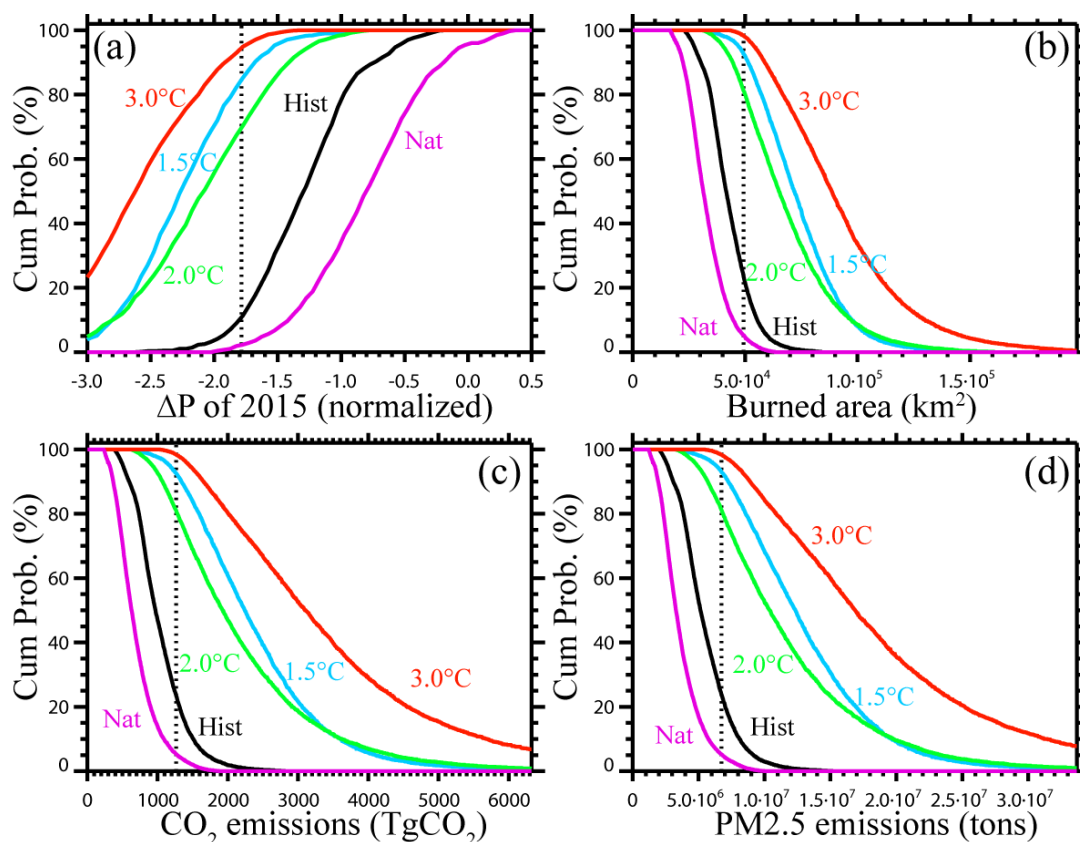


Figure 6: Surface air temperature warming patterns. (a)  $\Delta T$  differences between 3.0 °C and Nat (°C). The 30°S-30°N ocean averaged value is omitted. The black box indicates the Niño 3.4 region. The other panels are the same as panel (a) but for (b) 2.0 °C minus Nat, (c) 1.5 °C minus Nat and (d) Hist minus Nat.

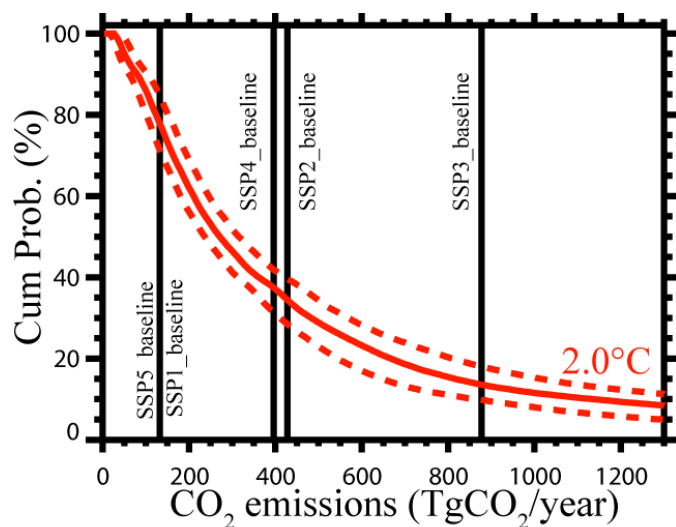


380 Figure 7: Relationships between Nino 3.4 warming and EA vertical motion and precipitation anomalies of the ensemble mean. The horizontal axes show differences in the 2015 T anomalies between the Nino 3.4 area and the 30°S-30°N ocean (°C). The vertical axes are (a)  $\Delta\omega_{500}$  (no unit) and (b)  $\Delta P$  (no unit) for the year 2015. Crosses denote the ensemble averages of Nat (purple), Hist (black), 1.5°C (light blue), 2.0°C (green) and 3.0°C (red).



385 **Figure 8.** Changes in the cumulative probability functions. (a) The vertical axis indicates the probability (%) of  $\Delta P$  being lower  
than a given horizontal value (no unit). Solid lines denote the 50% values of the 1000-random-samples of the Nat (purple), Hist  
(black), 1.5°C (light blue), 2.0°C (green) and 3.0°C (red) ensembles. The vertical dotted line is the observed 2015 value. The other  
panels show the probabilities of exceeding the given horizontal values for (b) the burned area ( $\text{km}^2$ ), (c)  $\text{CO}_2$  emissions ( $\text{TgCO}_2$ )  
and (d)  $\text{PM}_{2.5}$  emissions (tons).

390



395 Figure 9: The red curves are the cumulative probability function of CO<sub>2</sub> emissions (TgCO<sub>2</sub>/year) during the June-November 2006-2016 for the 2.0°C runs. Solid and dashed lines denote the 50% values and the 10-90% confidence intervals, respectively. The vertical lines indicate the year 2100 annual land-use CO<sub>2</sub> emission scenarios (including fire emissions) for the East and South East Asia region, except China and Japan for the 5 SSP baseline scenarios of the AIM/CGE model.